



An Evaluation of Dry, pCAM-free Cathode Synthesis Technology on Mid-Nickel $\text{LiNi}_{0.6}\text{Mn}_{0.2}\text{Co}_{0.2}\text{O}_2$ (NMC622) at the Pilot Scale

Van At Nguyen, Susi Jin, Nutthaphon Phattharasupakan, Akhil M. Abraham, Ryan I. Fielden, Mark A. McArthur¹

Dryve Battery Materials Inc., 110 Simmonds Drive, Dartmouth, Nova Scotia, B3B 1N9, Canada

The predicted exponential growth of electric vehicles and energy storage systems in North America necessitates the development of a robust domestic supply chain for lithium-ion battery components, particularly cathode active materials (CAMs). NOVONIX has developed an innovative dry, pCAM-free cathode synthesis process that eliminates the co-precipitation step, significantly reducing water usage, waste, and costs. This method simplifies the production flow, decreases unit operations, and lowers power consumption, potentially offering a 30% reduction in capital expense intensity and nearly 50% lower (excluding feedstock) processing costs compared to conventional cathode synthesis routes. NOVONIX's single crystal $\text{LiNi}_{0.6}\text{Mn}_{0.2}\text{Co}_{0.2}\text{O}_2$ (NMC622), synthesized via the dry, pCAM-free process, exhibits comparable electrochemical performance to commercially produced single crystal NMC622. Full-cell battery testing indicates competitive discharge capacity (Q_d), first cycle efficiency (FCE), gas evolution, and long-term cycling stability. These suggest that the dry, pCAM-free process is viable for producing high-quality NMC CAMs while presenting significant environmental and economic advantages. Further exploration and application of this technology to other cathode chemistries could play a critical role in developing a sustainable and cost-effective domestic and worldwide supply chain for lithium-ion batteries.

The demand for electric vehicles (EVs) and energy storage systems (ESS) in North America has grown rapidly in recent years. To prepare for this upcoming large-scale electrification, a strong domestic supply chain of battery materials and components for lithium-ion (Li-ion) batteries must be built. One of the most important components of Li-ion batteries is the cathode active material (CAM), which accounts for around 30% to 45% of the total cost structure of a Li-ion battery cell.^{1,2} There are two dominant CAM chemistries in use for EV and ESS applications; these are the nickel-containing oxide (e.g., lithium nickel manganese cobalt oxide (NMC)) or iron phosphate (e.g., lithium iron phosphate (LFP)) classes of materials. Compared to LFP, NMC stands out as having significantly higher energy density coupled with a long cycle life.^{3,4} Long cycle life and high energy density are both important when considering the requirements of domestic EVs. However, most CAM production is located outside North America and Europe.^{5,6} This leads to issues of national security, adds to logistics/handling costs, and increases environmental impact. Therefore, building NMC production capability in North America and Europe is a critical step in the supply chain.

A conventional route for producing NMC includes the synthesis of $\text{Ni}_x\text{Mn}_y\text{Co}_{1-x-y}\text{OH}$ precursor cathode active materials (pCAMs) from transition metal sulphate salts by co-precipitation, calcining pCAMs together with lithium a source at elevated temperatures, and applying any post-treatment or finishing processes. There are several concerns regarding the conventional production process of NMC CAM which are mainly related to the pCAM co-precipitation process. Firstly, a large volume of water is required in the synthesis of NMC pCAM. This inevitably leads to wastewater generation containing unreacted heavy metals, among other reagent chemicals, that need to be treated before discharging into the environment.⁷ Secondly, due to the use of sulphate feedstocks in co-precipitation, significant byproducts are produced, including sodium sulphate. In fact, it is estimated that for every tonne of pCAM produced, 1-3 tonnes of sodium sulphate are generated.⁷ Sodium sulphate byproduct can be sold into

secondary markets such as filler in powder laundry detergent, paper production, or glass making; however, its generation will quickly surpass the capacity requirements of these industries. Therefore, careful consideration must be given to the disposal or storage of sodium sulphate.⁸⁻¹⁰ Thirdly, co-precipitation requires a significant areal footprint to produce pCAM. This requirement leads to possible plant space constraints when co-located alongside CAM facilities: leading to increased production time, shipping logistics, and operating costs.

The concerns above, in addition to economic and environmental pressures in North America and Europe, must be considered carefully within the context of the domestic supply chain. Therefore, simplifying production steps and reducing waste generation are of utmost importance. Recently, several studies have focused on the synthesis of NMC using alternative processes.¹¹⁻¹⁴ These highly specialized "co-precipitation-free" methods can produce CAM with the trade-off of process complexity or the requirement of bespoke equipment. Since 2020, Dryve Battery Materials (Dryve) has been improving its patented cathode synthesis technology, deemed the dry, pCAM-free cathode production process, which is based on all-solid-state synthesis, to make NMC CAM.¹⁵⁻¹⁷ Following the work done by Lituo Zheng et al.,¹⁵ other labs around the world have also demonstrated that excellent NMC materials can be made using dry, pCAM-free methods, so it is clear that the method works well.¹⁸⁻²⁰ In contrast to other "co-precipitation-free" methods, the Dryve dry, pCAM-free cathode synthesis process results in a significant reduction in complexity and a simplification in production equipment. By avoiding the use of co-precipitation, process water can be eliminated in NMC CAM production. Moreover, a significant reduction of product waste is achieved by recycling fines generated during the deagglomeration step into the initial feedstock combination step (an efficiency not possible in the conventional cathode production process). Dryve engaged with Hatch Ltd. to perform an independent engineering report comparing the dry, pCAM-free process to conventional NMC CAM

¹E-mail: mark.mcarthur@dryvematerials.com

production.^{21,22} Based on their report, the dry, pCAM-free cathode production process has the potential to reduce capital expense intensity by nearly 30% and lower processing costs by nearly 50%. This can be done by simplifying the process flow, reducing unit operations, and decreasing power consumption requirements by an estimated 27% compared to the conventional cathode production process.

Dry, pCAM-free cathode synthesis excels at the production of NMC CAMs with single crystal (SC) morphology. Traditional NMC CAMs have polycrystalline (PC) morphology, which composes a plurality of sub-micron single crystal particulates agglomerated to form micron-size secondary particles. This morphology is prone to intragranular cracking after repeated charge/discharge cycling due to cathode volume expansion.²³ Those cracks allow more electrolyte species to infiltrate the core of PC particles where no protective coating is available. As a result, PC CAMs experience accelerated degradation causing rapid capacity fade.²⁴ SC NMC CAMs, in contrast, comprise micron-size, well-separated single crystal particulates that are more stable, mitigating particle cracking. Many studies suggest that well-designed Li-ion batteries with SC NMC CAMs could last a very long time under aggressive environmental and electrochemical conditions.^{4,25}

The Dryve dry, pCAM-free process is compatible with a range of NMC chemistries, including mid-nickel (50-60% Ni) to high nickel (>80% Ni) and low or no cobalt formulations. Cobalt-free formulations are unique in that they eliminate much of the ethical considerations associated with some critical mineral extraction and mitigating costs by substitution with lower-cost materials. In this white paper, our focus is the demonstration of mid-nickel SC LiNi_{0.6}Mn_{0.2}Co_{0.2}O₂ (NMC622) CAM produced by dry, pCAM-free technology to demonstrate its competitive performance versus conventionally made NMC622 CAM in lithium-ion batteries.

Experimental

Material Synthesis.—Dryve NMC622 was prepared by a dry, pCAM-free process. First, stoichiometric amounts of transition metal feedstocks were combined with Li₂CO₃ in a single step. Transition metal feedstock materials could be selected from groups of metal powders, oxide powders, carbonate powders, or combinations thereof. Approximately 4 kg of the combined feedstock was treated and loaded into each standard ceramic sagger (330 mm x 330 mm x 100 mm). Saggars were loaded in a 2 x 2 configuration into a 13.5 m, 16-zone roller hearth kiln (RHK). The total amount of feedstock for this run was 120 kg and calcination was performed under flowing oxygen gas. The calcined product was first coarsely crushed by roller crusher (300 kg/h) and further deagglomerated by jet milling (100 kg/h) to yield pristine NMC622 CAM. Pristine NMC622 underwent several post-treatment processes familiar to conventional cathode processing, however, in a completely dry state. These included thermal and coating treatments. A commercial SC NMC622 CAM sourced from a reputable vendor which was made by conventional processes was used as a reference.

Material characterization.—Material characterization was performed using Dryve’s analytical laboratory. Measurements included scanning electron microscopy coupled with energy-dispersive x-ray spectroscopy (SEM/EDX; Thermo Fisher Scientific, Phenom XL G2) for morphology and bulk elemental mapping,

powder x-ray diffraction (XRD; Bruker D8 Discover with LYNXEYE detector) for crystallinity measurement, laser-scattering particle size distribution analysis (PSD; Horiba LA-950V2) for particle size measurement, automatic titration (AT; Mettler Toledo, Titrator Excellence T5) for surface lithium residuals quantification, and inductively coupled plasma-optical emission spectroscopy (ICP-OES; Agilent, 5800 VDV) for elemental composition and impurity quantification. Transmission electron microscopy coupled with energy-dispersive x-ray spectroscopy (TEM/EDX; Thermo Fisher Scientific, Talos 200X) was performed at the Canadian Centre for Electron Microscopy (CCEM, McMaster University) to evaluate elemental distribution of NMC materials.

Electrochemical characterization.—Coin cell evaluation of Dryve and commercial SC NMC622 CAMs was performed in CR2032 format coin half-cells at Dryve’s R&D facilities. Cathode slurries were mixed using a planetary mixer (Mazerustar KK-250) with a composition of 94/4/2 wt.%: CAM/carbon black (Imerys Timcal Super P Li)/polyvinylidene fluoride (PVDF) binder (Solvay Solef 5130) in N-methyl-2-pyrrolidone (NMP) solvent (Univar Solutions; target slurry solids content of 50 wt.%). Cathode slurries were cast onto 15 μm aluminum foil by doctor blade. Target cathode areal mass loadings and compression densities were approximately 21 mg/cm² and 3.0 g/cm³, respectively. CR2032 coin cells were fabricated in an argon-filled glovebox with oxygen and moisture contents below 1 ppm. An electrolyte consisting of 1.2 M lithium hexafluorophosphate (LiPF₆) in an ethylene carbonate (EC): ethylmethyl carbonate (EMC): dimethyl carbonate (DMC) (25:5:70 wt.%) solvent blend was used. Galvanostatic cycling measurements were performed using battery cyclers (Neware MIHW-200-160CH) at 25.0°C. Coin cell cycling was done between 2.8-4.5 V with the following protocol: Cycles 1 and 2 at constant current (CC) of 0.05C followed by a constant voltage (CV) hold at top of charge until the current decayed to 0.02C; Cycles 3 onwards at CC rate of 0.2C.

Table 1. Design parameters for 1 Ah stacked pouch cells balanced to 4.3 V using artificial graphite anode and NMC622 cathode powders.

Parameter	Anode	Cathode
foil	10 μm Cu	15 μm Al
electrode thickness (μm; single side)	81	65
mass loading (mg/cm ²)	12.54	21.45
reversible areal capacity (mAh/cm ²)	4.040	3.661
compression density (g/cm ³)	1.55	3.3
electrode number in 1 Ah	7	6
effective N/P ratio	1.07	

Full pouch-type Li-ion cells (containing both CAM and graphite anode) were made at Avrion Lab’s cell prototyping and testing facilities (177 Bluewater Rd, Bedford, NS). Table 1 shows some of the properties of 1 Ah stacked pouch cell balanced to 4.3 V designed for this study. The cathode and anode materials were coated by slot-die on a roll-to-roll coater (4 m drier zone). The cathode coating formulation was 94/4/2 wt.%: CAM/carbon black (Imerys Timcal Super P Li)/ PVDF binder (Solvay Solef 5130). The anode coating formulation was 94.5/1.3/1.4/2.8 wt.%: artificial graphite (Kajin AML400)/carbon black (Imerys Timcal Super P Li)/carboxymethyl cellulose (CMC; Nippon Paper Sunrose MAC

350HC)/styrene butadiene rubber (SBR; Zeon BM-451B). After drying, multi-layer pouch cells were assembled in a humidity-controlled dryroom (dewpoint < -40°C). Assembly was done on a semi-auto electrode stacking machine, alternating 7 and 6 layers of double-sided coated anode and cathode electrodes, respectively. It is possible that these outer electrodes can result in reduced electrochemical performance and are a consequence of cell assembly.²⁶ Electrode areal capacity loadings were selected to give an effective negative-to-positive ratio (N/P) of 1.07 (total N/P would be significantly larger due to the anode coatings facing the outside of the stack). Pouch cells were filled with 3 mL/Ah of electrolyte consisting of 1.2 M LiPF₆ in EC:EMC:DMC (25:5:70

wt.%) with 3 wt.% vinylene carbonate (VC). After filling cells were fixtured at 67 kPa (10 psi) for formation and long-term cycling. All cells underwent a formation protocol at 40.0°C consisting of:

- a 24 h voltage hold at 1.5 V to improve electrolyte wetting,
- a CC charge/discharge cycle at 0.05C between 4.3-3.0 V,
- a CC charge to 4.3 V at 0.05C followed by a 48 h rest step at top of charge, and
- a CC discharge to 60% state of charge (SOC) for post formation measurements.

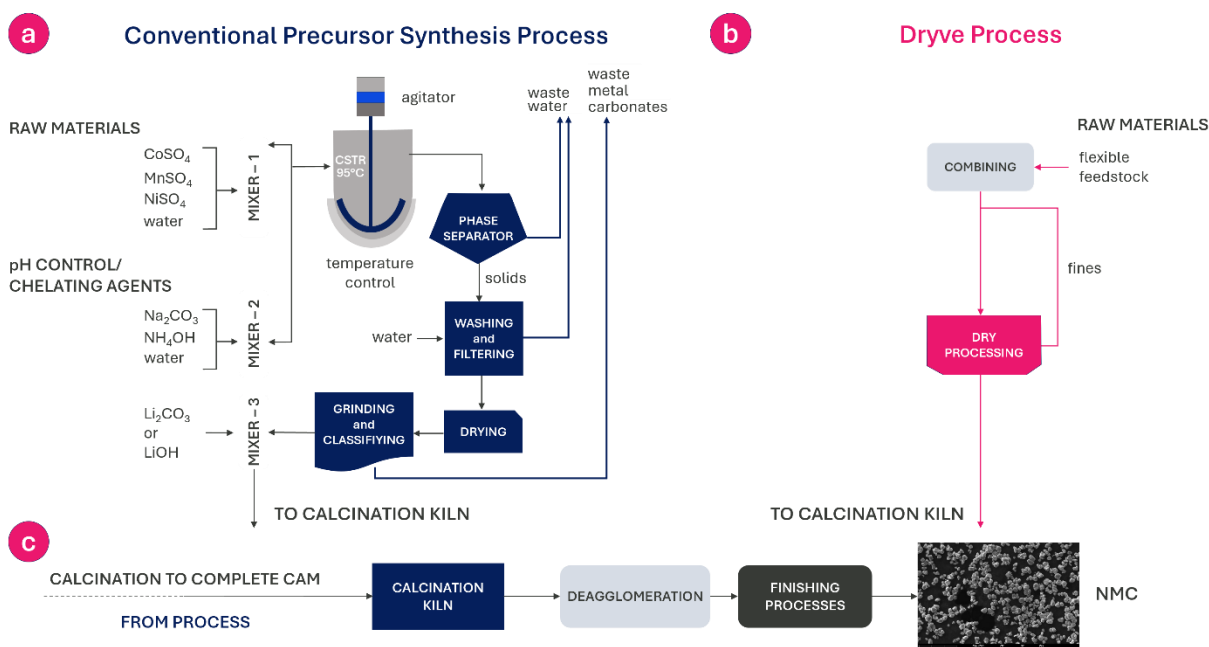


Figure 1. Process flow diagrams of (a) conventional pCAM synthesis, (b) Drye dry, pCAM-free CAM synthesis, and (c) common calcination process for producing NMC CAM powders.

Volume change measurements were performed on each cell using the Archimedes' principle to estimate the gas evolved during formation.²⁷ The cells were then degassed and resealed under vacuum in the dry room. Post formation cycle aging tests were conducted at room temperature (~22°C) and 40°C. At 40°C, cells were cycled at a rate of CC-0.33C with CV-0.05C on charge. Similarly at room temperature, cells were cycled at a rate of CC-1C with CV-0.05C on charge.

Results and Discussion

Figure 1 shows a schematic diagram of the conventional and the dry, pCAM-free CAM synthesis processes. Conventional NMC synthesis is complex and requires the production of a pCAM powder (Figure 1a). During the production of pCAM powder (typically Ni_xMn_yCo_{1-x-y}OH), transition metal sulphate salts are dissolved in water and then precipitated in a reaction mediated by pH-controlling (e.g., acids/bases) and chelating agents (e.g., ammonium hydroxide (NH₄OH)) in a continuous stirred tank reactor (CSTR) at elevated temperature (e.g., 95°C). The co-

precipitated precursors are then separated from unreacted raw materials and solvents, washed, dried, and ground into fine powder. pCAM powder synthesis consumes vast quantities of fresh water and generates correspondingly significant amounts of wastewater (3,500-15,000 L per tonne NMC) and byproducts, including sodium sulphate (NaSO₄; 1-3 tonnes per tonne NMC).⁷ These waste products require treatment and disposal processes. Following co-precipitation (Figure 1c), pCAM powders are then mixed with a lithium source (e.g., lithium carbonate (Li₂CO₃) or hydroxide (LiOH)) before calcination in a RHK at temperatures in excess of 800°C. In contrast to conventional processes, Drye dry, pCAM-free processing has fewer steps (Figure 1b). Stoichiometric amounts of transition metal feedstocks, including, but not limited to, metals, oxides, carbonates, or mixtures thereof, are combined directly together with lithium sources and dopants in a single step prior to calcination (Figure 1c). This calcination step, and its conditions, are near-identical to conventional NMC calcination and require no new specialized equipment. After calcination, CAM powders are deagglomerated and possibly post-treated.

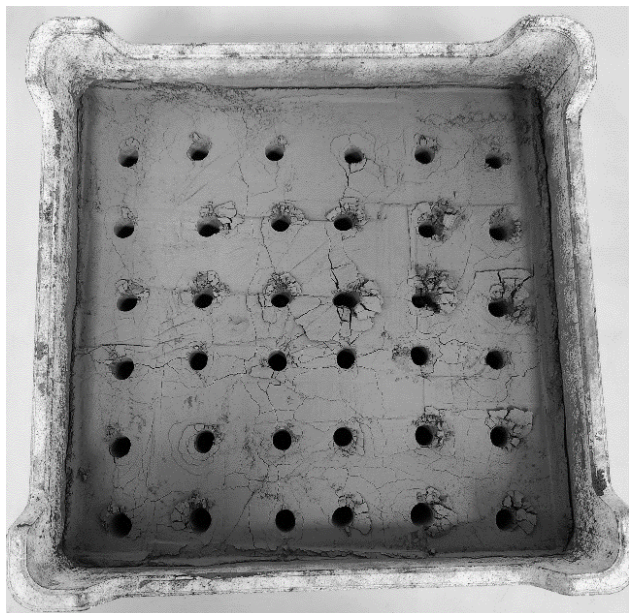


Figure 2. A ceramic sagger loaded with powders after the Dryve dry, pCAM-free process ready for calcination to generate single crystal NMC622 powders.

Figure 2 shows a photograph of a standard 330 mm x 330 mm x 100 mm ceramic sagger loaded with combined powders (Ni, Mn, Co, Li, and dopants) after dry, pCAM-free processing and before calcination in order to synthesize NMC622. The sagger mass loading was 4 kg, which could be increased further to above 5 kg to improve production throughput (limited by sagger dimensions). Mechanical holes were made in the powder bed after tamping by hand to improve gas circulation during calcination. Figure 3a shows a photograph of the end sections of the 13.5 m long RHK with several heat-insulative panels temporarily removed. Figure 3b shows the loading geometry of saggars in a stacked 2 x 2 configuration within the RHK.

Figure 4 shows SEM images of Dryve NMC622 (Figures 4a and b) and commercial NMC622 powders (Figures 4c and d), which

have similar single-crystal morphology. For the Dryve NMC622 CAM, a simple aluminum oxide (Al_2O_3) surface coating was applied in a dry state using nano-sized aluminum oxide. As part of the finishing process, the sample was refired to stabilize the surface. The finishing processes utilized in the synthesis of the commercial NMC622 powder were unknown; however, we can infer by ICP-OES that there was a surface coating present (data not shown). Figure 5 shows powder XRD patterns for both Dryve and commercial NMC622. Both materials exhibited an O3-layered structure with comparable crystallinity. No evidence of phase impurities was found, indicating that the dry, pCAM-free process is capable of producing pure-phase NMC CAM powders comparable to commercially accepted materials.

As mentioned above, commercial NMC powders are produced via conventional processes, i.e., conversion of a pCAM from wet chemistry, combined with lithium, and calcined into a CAM (Figures 1a and c). The perceived benefit of co-precipitated pCAM is good intraparticle homogeneity after calcination.²⁸ Unlike the conventional method, dry, pCAM-free processing eliminates the pCAM synthesis route and relies upon the formation of a solid solution to intimately combine the transition metals, lithium, and any dopants in a single step. Several studies have described strategies to overcome the inherent challenge of solid-state methods, which is the compositional inhomogeneity of NMC materials, through wet ball milling.^{29,30} However, wet ball milling requires specialized milling equipment and results in low production throughput. Tahmasebi et al. demonstrated the importance of compositional homogeneity on the performance of NMC materials made by solid-state methods.³¹ Therefore, it was necessary for us to demonstrate at pilot scale that the Dryve dry, pCAM-free process can produce NMC powders with excellent intraparticle homogeneity with no localized elemental concentrations, i.e., elemental islanding. Figures 6 and 7 show SEM/EDX and higher resolution transmission electron microscopy/energy dispersion x-ray spectroscopy (TEM/EDX) mapping of several representative particles of both Dryve and commercial NMC622, respectively, to evaluate the elemental distribution of constituent elements. TEM/EDX measurements were performed by an external partner organization.



Figure 3. Photograph of the Dryve 13.5 m long RHK with insulating covers removed showing gas handling system and roller/heater covers (a) and sagger arrangement within the RHK entering the kiln ‘hot zone’ (b).

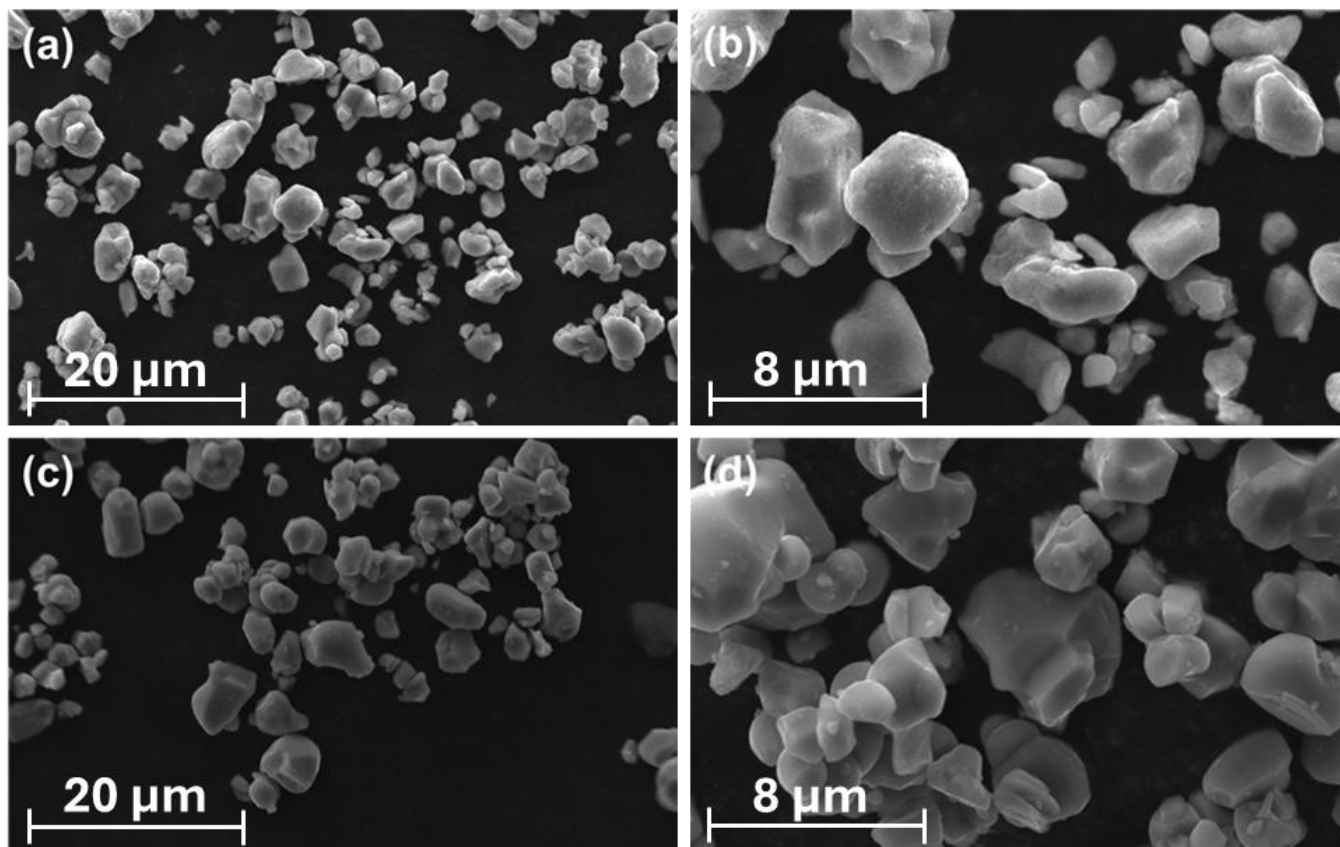


Figure 4. SEM images of (a, b) single-crystal NMC622 produced via dry, pCAM-free processing (Dryve NMC622) and (c, d) conventionally made commercial single-crystal reference NMC622 powder.

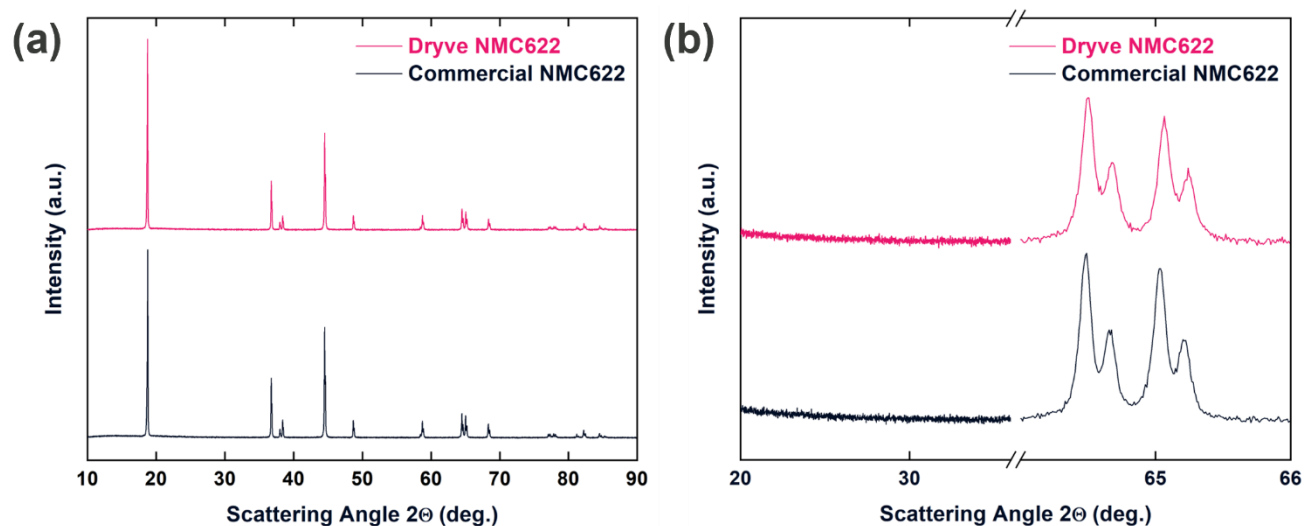


Figure 5. Powder XRD patterns of Dryve NMC622 and commercial NMC622 for (a) full view (10-90° 2θ) and (b) expanded views of impurity region (20-30° 2θ) and (018)/(110) peak region (64-66° 2θ).

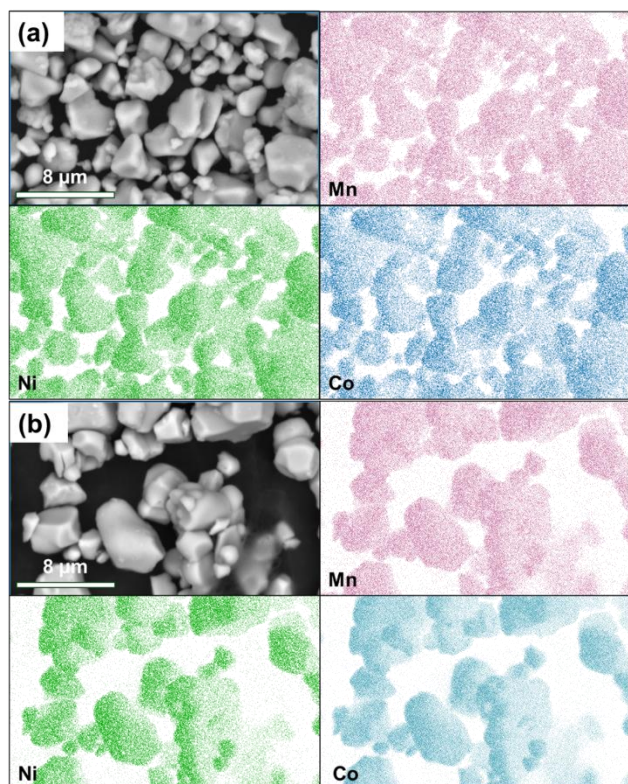


Figure 6. Elemental distribution by SEM/EDX of (a) Dryve NMC622 and (b) commercial NMC622.

The colour mapping quantifies the intensity of the indicated elements. At the resolution of both the SEM and the TEM, the elemental maps show that both the Dryve and commercial NMC622 powders have good intraparticle homogeneity which is expected to deliver good cycle life performance.

Table 2 compares measured properties of the Dryve NMC622 and commercial NMC622 CAMs. It is important to note that iron was not removed from the Dryve NMC622 sample. In fact, based on the stoichiometry and impurities of the material feedstock, iron content is expected to be less than 10 ppm. The relatively high iron concentration has been identified as originating from our deagglomerating process, i.e., the jet milling step. More aggressive iron removal controls are expected to be in place for future sample batches. The surface area of Dryve NMC622 is slightly higher compared to the commercial NMC622. This can be attributed to the dry coating process during material finishing, and it can be tailored depending on the end application for the material.

To compare the CAM-specific electrochemical performance of Dryve NMC622 with commercial NMC622, coin half-cells were constructed and tested. Figures 8a and b show that Dryve NMC622 has competitive discharge capacity and retention after 50 cycles at a rate of 0.2C between 2.8-4.5 V. These data demonstrate that NMC622 produced via dry, pCAM-free methods is competitive to commercial NMC622 made by conventional processes.

Pouch cells were made with either commercial NMC622 or Dryve NMC622 and graphite anode in order to understand how each cathode behaved in a typical lithium-ion battery configuration. Figures 9a and b summarize the first cycle efficiency (FCE) and evolved gas volume after cell formation of both the Dryve NMC622/graphite and commercial NMC622/graphite cell types.

Dryve NMC622/graphite cells exhibited competitive FCE and gas evolution during formation relative to cells containing commercial cathode materials. It is unsurprising that the commercial NMC622 has slightly superior FCE and lower gas generation than Dryve NMC622. This commercial powder is fully optimized and device-ready. Dryve NMC622 was made with very few dopants and finished using a simple coating. These formation data are encouraging and with further optimization, future Dryve powders are expected to meet or exceed the commercial cathode's electrochemical performance.

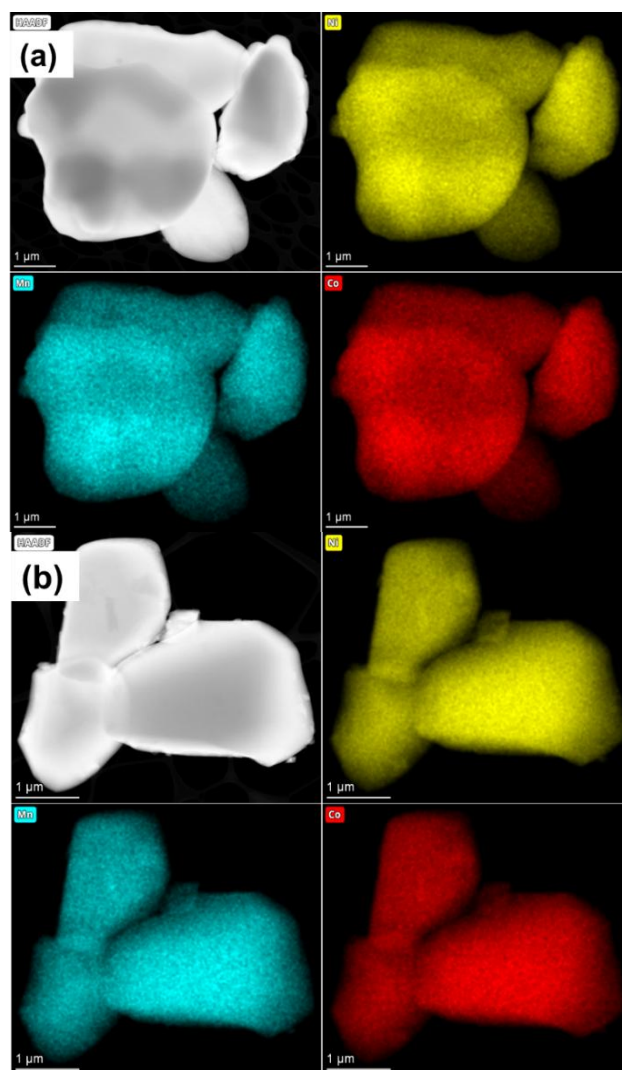


Figure 7. Elemental distribution by TEM/EDX of (a) Dryve NMC622 and (b) commercial NMC622.

Figures 10a and b show normalized discharge (a) and charge (b) rate mapping for cells containing either Dryve or commercial NMC622 cathodes. Dryve NMC622 cells show competitive rate capabilities relative to commercial cathode of the same chemistry. This helps further demonstrate the compatibility of Dryve cathode materials with existing testing and cell building practices.

Figures 11a and b show normalized discharge capacity and ΔV (the difference in charge and discharge voltage normalized to cycle one, an indicator of impedance growth) of 1 Ah stacked pouch cells cycled at 40°C at current rates of 0.33C. The capacity retention of

Dryve NMC622/graphite cells is competitive with commercial NMC622/graphite full cells after more than 500 cycles. Impedance growth of both cell types is similar over the same period. The stability of the Dryve NMC622 cathode is competitive to commercial cathode materials. Additional electrolyte formulations, including advanced electrolyte beyond 3 wt.% VC, are expected to greatly improve cycle life and suppress polarization growth.

Figures 12a and b show normalized capacity and ΔV of 1 Ah stacked cells cycled at room temperature and 1.0C rates. Under these conditions, cells containing Dryve NMC622 perform similarly to commercial NMC622 cathode powders.

Full cells in this study were made by alternating layers of double-sided electrode sheets in a stack (6 cathode and 7 anode layers). The outer layers are the anode electrodes. Because these outer layers are double-side coated, it is possible that lithium from the cathode can migrate into the graphite that is not facing cathode on the outward side of the layer during charge. The effect of such

‘book ending’ may result in the loss of lithium inventory through SEI formation and lithium trapping that could cause faster capacity fade.²⁶ Improvements to the cell design, e.g., single-sided outer anode electrodes or larger capacity cell designs with double-sided outer electrodes, could improve full-cell cycle life performance for both Dryve NMC622 and commercial NMC622.

Further optimization to the finishing processes is expected to close any gaps in performance for FCE, gas generation, rate testing, and ΔV observed between the Dryve and commercial materials. Optimization could include, but is not limited to, specialized dopant and coating combinations, additional post-heat treatment steps, or judicious washing with water (undesirable for a dry process). Based on these data, one can conclude that Dryve dry, pCAM-free cathode synthesis technology can generate a class of single-crystal mid-nickel NMC with competitive performance to commercial CAMs for the EV and ESS battery sectors.

Table 2. Properties of Dryve NMC622 and commercial NMC622. The terminology <MDL indicates that the elemental concentration is less than the minimum detection limit of our ICP-OES instrument. *No iron removal was performed on the Dryve NMC622 sample.

Item	Description	Unit	Measurement	
			Dryve NMC622	Commercial NMC622
chemistry	Ni	mol.%	60.5 ± 0.7	60.6 ± 0.6
	Mn	mol.%	19.8 ± 0.1	19.6 ± 0.2
	Co	mol.%	19.7 ± 0.2	19.8 ± 0.2
	Li	wt.%	8.7 ± 0.1	7.9 ± 0.1
impurities	Ca	ppm	<MDL	<MDL
	Cu	ppm	<MDL	<MDL
	Fe	ppm	63 ± 1*	<MDL
	Na	ppm	79 ± 9	61 ± 9
	Si	ppm	<MDL	46.7 ± 0.8
	Zn	ppm	<MDL	<MDL
lithium residuals	LiOH	ppm	870 ± 50	1400 ± 100
	Li ₂ CO ₃	ppm	480 ± 50	1830 ± 80
BET surface area		m ² /g	0.9 ± 0.1	0.7 ± 0.1
PSD	D10	μm	2.5 ± 0.1	3.1 ± 0.1
	D50	μm	3.8 ± 0.1	4.8 ± 0.1
	D90	μm	5.6 ± 0.1	7.1 ± 0.4
coin half-cell (0.05C; 2.8-4.5V; 25°C)	Q _d	mAh/g	196.5 ± 0.5	196.3 ± 0.6
	FCE	%	88.8	87.6

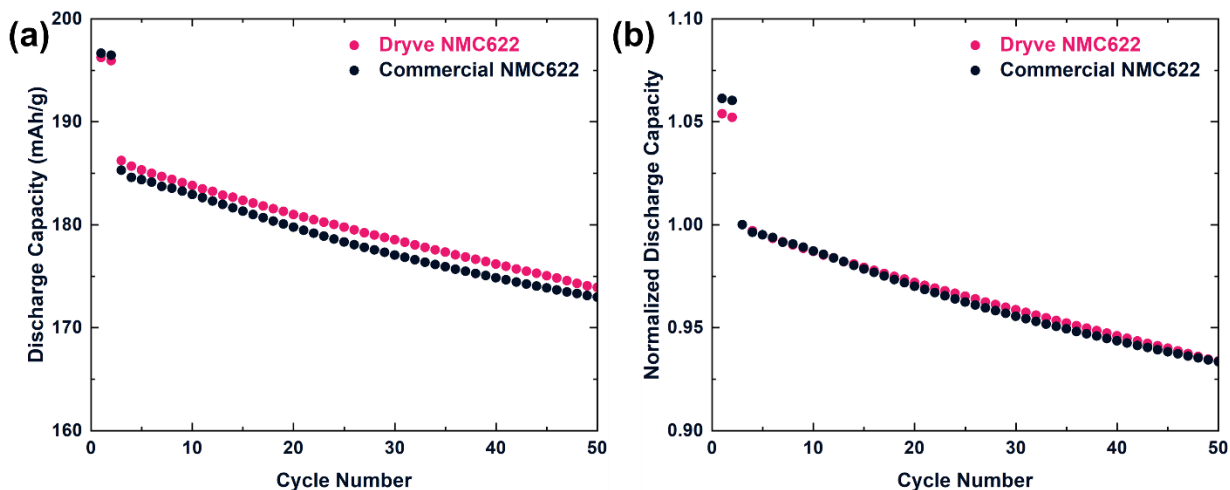


Figure 8. Electrochemical testing of coin half-cells with commercial and Dryve NMC622 showing (a) discharge capacity with cycling between 2.8-4.5 V at CC-0.05C (Cycles 1 and 2) and CC-0.2C (Cycles 3+) and (b) normalized discharge capacity from (a).

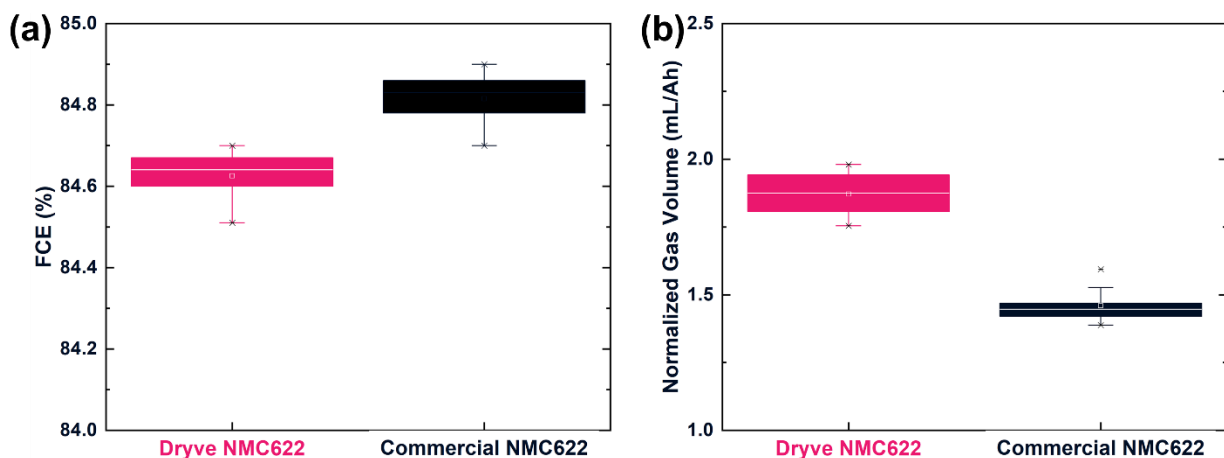


Figure 9. First cycle coulombic efficiency (FCE) (a) and capacity-normalized gas volume after formation (b) for Dryve NMC622/graphite and commercial NMC622/graphite full cells.

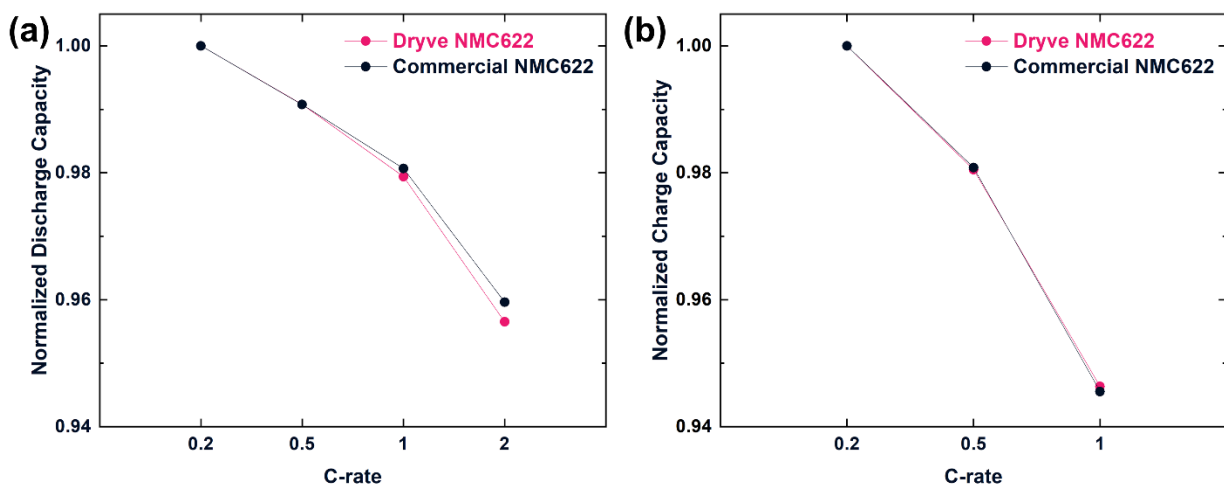


Figure 10. Normalized charge (a) and discharge (b) capacities of 1 Ah pouch cells containing either Dryve or commercial NMC materials as a function of C-rate between 3.0-4.3 V at 40°C.

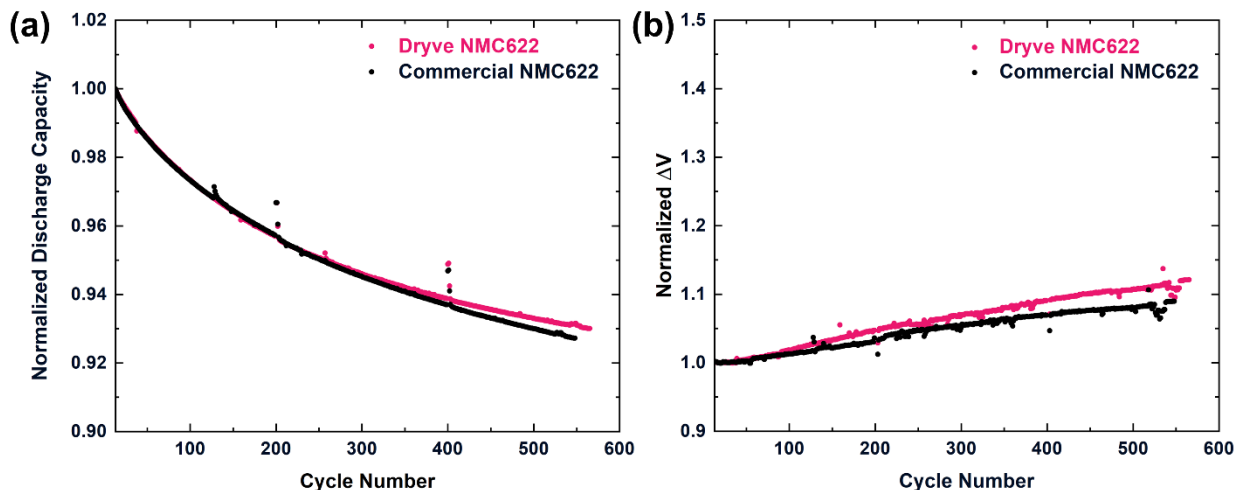


Figure 11. Normalized discharge capacity (a) and ΔV (b) of long-term cycling of 1 Ah pouch cells containing Dryve or commercial NMC622 cycled between 3.0-4.3V at CC-0.33C and 40°C.

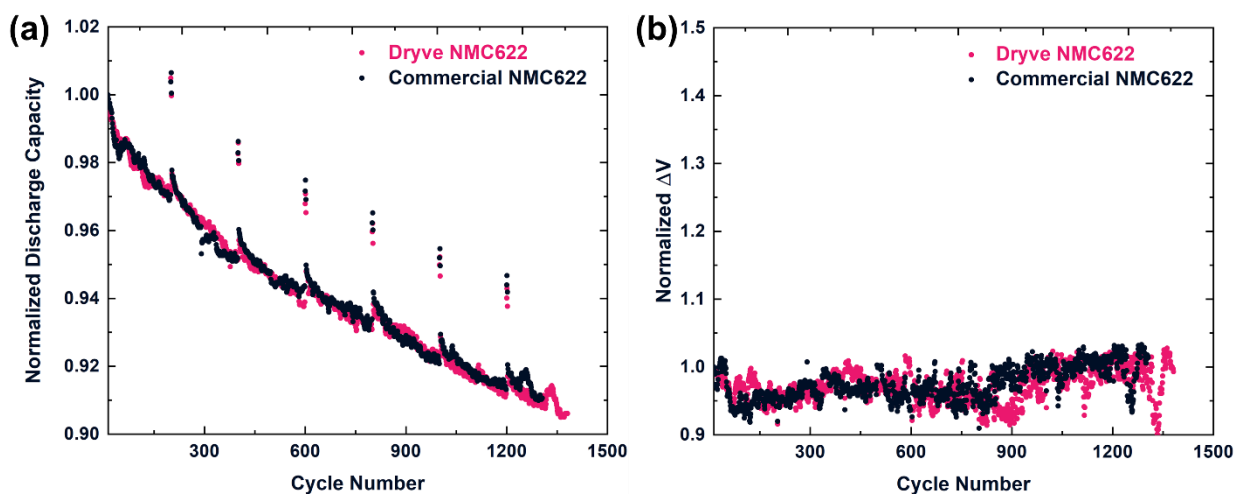


Figure 12. Normalized discharge capacity (a) and ΔV (b) of long-term cycling of 1 Ah pouch cells containing Dryve or commercial NMC622 cycled between 3.0-4.3V at CC-1.0C and room temperature (~22°C).

Conclusion

Dryve Battery Materials has demonstrated that high quality NMC622 cathode powders can be synthesized using its patented dry, pCAM-free processes in its pilot demonstration facility. Most importantly, these materials exhibit competitive performance to commercial NMC622 powders. Modification of the base CAM, e.g., finishing via surface coating optimization, is anticipated to further improve its physical and electrochemical characteristics. It is our recommendation that all-dry processing technology, such as the Dryve dry, pCAM-free cathode synthesis process, should be further explored and applied to additional cathode chemistries. Processing CAM in a dry state has numerous economic and environmental advantages to conventional cathode production and generates ‘drop-in ready materials’. Ultimately, NMC622 produced utilizing Dryve’s technology can play an important role in decreasing production costs and reducing waste while maintaining material performance in domestic corridors.

It is very likely as CAM plants are built and scaled to be larger (>100,000 tpa) that permitting for water use and waste disposal at such scale will be impossible, even in traditional jurisdictions such as Asia. The Dryve dry, pCAM-free process described here is the solution for scaling CAM production.

References

- (1) AVICENNE ENERGY. *The Rechargeable Battery Market and Main Trends 2020-2030*; 2021. <https://www.avicenne.com> (accessed 2024-07-16).
- (2) Wentker, M.; Greenwood, M.; Leker, J. A Bottom-up Approach to Lithium-Ion Battery Cost Modeling with a Focus on Cathode Active Materials. *Energies (Basel)* **2019**, *12* (3). <https://doi.org/10.3390/en12030504>.
- (3) Aiken, C. P.; Logan, E. R.; Eldesoky, A.; Hebecker, H.; Oxner, J. M.; Hartow, J. E.; Metzger, M.; Dahn, J. R. $\text{Li}[\text{Ni}_{0.5}\text{Mn}_{0.3}\text{Co}_{0.2}]\text{O}_2$ as a Superior Alternative to LiFePO_4 for Long-Lived Low Voltage Li-Ion

- Cells. *J Electrochem Soc* **2022**, 169 (5), 050512. <https://doi.org/10.1149/1945-7111/ac67b5>.
- (4) Li, J.; Cameron, A. R.; Li, H.; Glazier, S.; Xiong, D.; Chatzidakis, M.; Allen, J.; Botton, G. A.; Dahn, J. R. Comparison of Single Crystal and Polycrystalline $\text{LiNi}_{0.5}\text{Mn}_{0.3}\text{Co}_{0.2}\text{O}_2$ Positive Electrode Materials for High Voltage Li-Ion Cells. *J Electrochem Soc* **2017**, 164 (7), A1534–A1544. <https://doi.org/10.1149/2.0991707jes>.
- (5) Cheng, A. L.; Fuchs, E. R. H.; Karplus, V. J.; Michalek, J. J. Electric Vehicle Battery Chemistry Affects Supply Chain Disruption Vulnerabilities. *Nat Commun* **2024**, 15 (1). <https://doi.org/10.1038/s41467-024-46418-1>.
- (6) Gohlke, D.; Krishnamoorthy Iyer, R.; Kelly, J.; Pene, A.; Monthe, N.; Wu, X.; Mansour, C. Quantification of Commercially Planned Battery Component Supply in North America through 2035; 2024. <https://publications.anl.gov/anlpubs/2024/03/187735.pdf> (accessed 2024-07-16).
- (7) Ahmed, S.; Nelson, P. A.; Gallagher, K. G.; Susarla, N.; Dees, D. W. Cost and Energy Demand of Producing Nickel Manganese Cobalt Cathode Material for Lithium Ion Batteries. *J Power Sources* **2017**, 342, 733–740. <https://doi.org/10.1016/j.jpowsour.2016.12.069>.
- (8) Tuovinen, T.; Tynjälä, P.; Vielma, T.; Lassi, U. Utilization of Waste Sodium Sulfate from Battery Chemical Production in Neutral Electrolytic Pickling. *J Clean Prod* **2021**, 324, 129237. <https://doi.org/10.1016/j.jclepro.2021.129237>.
- (9) Karjalainen, J.; Hu, X.; Mäkinen, M.; Karjalainen, A.; Järvisjö, J.; Järvenpää, K.; Sepponen, M.; Leppänen, M. T. Sulfate Sensitivity of Aquatic Organism in Soft Freshwaters Explored by Toxicity Tests and Species Sensitivity Distribution. *Ecotoxicol Environ Saf* **2023**, 258, 114984. <https://doi.org/10.1016/j.ecoenv.2023.114984>.
- (10) Wang, N.; Dorman, R. A.; Ivey, C. D.; Soucek, D. J.; Dickinson, A.; Kunz, B. K.; Steevens, J. A.; Hammer, E. J.; Bauer, C. R. Acute and Chronic Toxicity of Sodium Nitrate and Sodium Sulfate to Several Freshwater Organisms in Water-Only Exposures. *Environ Toxicol Chem* **2020**, 39 (5), 1071–1085. <https://doi.org/10.1002/etc.4701>.
- (11) Chan, K. H.; Liu, H.; Azimi, G. Synthesis of a Nickel-Rich $\text{LiNi}_{0.6}\text{Mn}_{0.2}\text{Co}_{0.2}\text{O}_2$ Cathode Material Utilizing the Supercritical Carbonation Process. *Ind Eng Chem Res* **2023**, 62 (10), 4271–4280. <https://doi.org/10.1021/acs.iecr.2c04487>.
- (12) Ahn, W.; Lim, S. N.; Jung, K.-N.; Yeon, S.-H.; Kim, K.-B.; Song, H. S.; Shin, K.-H. Combustion-Synthesized $\text{LiNi}_{0.6}\text{Mn}_{0.2}\text{Co}_{0.2}\text{O}_2$ as Cathode Material for Lithium Ion Batteries. *J Alloys Compd* **2014**, 609, 143–149. <https://doi.org/10.1016/j.jallcom.2014.03.123>.
- (13) Guo, J.; Li, W. Synthesis of Single-Crystal $\text{LiNi}_{0.7}\text{Co}_{0.15}\text{Mn}_{0.15}\text{O}_2$ Materials for Li-Ion Batteries by a Sol-Gel Method. *ACS Appl Energy Mater* **2022**, 5 (1), 397–406. <https://doi.org/10.1021/acsaem.1c02939>.
- (14) Ajayi, B. P.; Thapa, A. K.; Cvelbar, U.; Jasinski, J. B.; Sunkara, M. K. Atmospheric Plasma Spray Pyrolysis of Lithiated Nickel-Manganese-Cobalt Oxides for Cathodes in Lithium Ion Batteries. *Chem Eng Sci* **2017**, 174, 302–310. <https://doi.org/10.1016/j.ces.2017.09.022>.
- (15) Lituo, Z.; Nikolas, O. M.; Sefid, D. M. H. T.; Laurie, C.; Barak, I. Ben. Methods for Preparing Lithium Nickel Manganese Cobalt Oxide Particulate. WO 2023230537 A1, 2023.
- (16) Lituo, Z.; Nikolas, O. M. Lithium Transition Metal Oxide and Precursor Particulate Materials and Methods. JP 7504195 B2, 2024.
- (17) Zheng, L.; Bennett, J. C.; Obrovac, M. N. All-Dry Synthesis of Single Crystal NMC Cathode Materials for Li-Ion Batteries. *J Electrochem Soc* **2020**, 167 (13), 130536. <https://doi.org/10.1149/1945-7111/abbc1>.
- (18) Zhang, N.; Yu, H.; Murphy, A.; Garayt, M.; Yu, S.; Rathore, D.; Leontowich, A.; Bond, T.; Kim, C.-Y.; Dahn, J. R. A Liquid and Waste-Free Method for Preparing Single Crystal Positive Electrode Materials for Li-Ion Batteries. *J Electrochem Soc* **2023**, 170 (7), 070515. <https://doi.org/10.1149/1945-7111/ace4f7>.
- (19) Garayt, M. D. L.; Zhang, N.; Yu, S.; Abraham, J. J.; Murphy, A.; Omessi, R.; Ye, Z.; Azam, S.; Johnson, M. B.; Yang, C.; Dahn, J. R. Single Crystal $\text{Li}_{1+x}[\text{Ni}_{0.6}\text{Mn}_{0.4}]_{1-x}\text{O}_2$ Made by All-Dry Synthesis. *J Electrochem Soc* **2023**, 170 (6), 060529. <https://doi.org/10.1149/1945-7111/acdd24>.
- (20) Yu, S.; Zhang, N.; Garayt, M.; Leslie, K.; Yang, C.; Dahn, J. R. All Dry in One Step (ADIOS to Water) Synthesis of W-Coated $\text{Li}_{1+x}(\text{Ni}_{0.7}\text{Mn}_{0.3})_{1-x}\text{O}_2$. *J Power Sources* **2023**, 581, 233432. <https://doi.org/10.1016/j.jpowsour.2023.233432>.
- (21) NOVONIX Announces Results of Engineering Study on Proprietary All-Dry, Zero-Waste Cathode Synthesis Process. <https://ir.novonixgroup.com/news-releases/news-release-details/novonix-announces-results-engineering-study-proprietary-all-dry> (accessed 2024-07-16).
- (22) NOVONIX PCAM & CAM Comparison Study: Conceptual Study Report; 2023.
- (23) Yoon, S.; Park, H. G.; Koo, S.; Hwang, J.; Lee, Y.; Park, K.; Kim, D. An In-Depth Understanding of Chemomechanics in Ni-Rich Layered Cathodes for Lithium-Ion Batteries. *J Alloys Compd* **2023**, 939, 168531. <https://doi.org/10.1016/j.jallcom.2022.168531>.
- (24) Hu, J.; Wang, H.; Xiao, B.; Liu, P.; Huang, T.; Li, Y.; Ren, X.; Zhang, Q.; Liu, J.; Ouyang, X.; Sun, X. Challenges and Approaches of Single-Crystal Ni-Rich Layered Cathodes in Lithium Batteries. *Natl Sci Rev* **2023**, 10 (12). <https://doi.org/10.1093/nsr/nwad252>.
- (25) Harlow, J. E.; Ma, X.; Li, J.; Logan, E.; Liu, Y.; Zhang, N.; Ma, L.; Glazier, S. L.; Cormier, M. M. E.; Genovese, M.; Buteau, S.; Cameron, A.; Stark, J. E.; Dahn, J. R. A Wide Range of Testing Results on an Excellent Lithium-Ion Cell Chemistry to Be Used as Benchmarks for New Battery Technologies. *J Electrochem Soc* **2019**, 166 (13), A3031–A3044. <https://doi.org/10.1149/2.0981913jes>.
- (26) Garayt, M. D. L.; Johnson, M. B.; Laidlaw, L.; McArthur, M. A.; Trussler, S.; Harlow, J. E.; Dahn, J. R.; Yang, C. A Guide to Making Highly Reproducible Li-Ion Single-Layer Pouch Cells for Academic Researchers. *J Electrochem Soc* **2023**, 170 (8), 080516. <https://doi.org/10.1149/1945-7111/aceffc>.
- (27) Aiken, C. P.; Xia, J.; Wang, D. Y.; Stevens, D. A.; Trussler, S.; Dahn, J. R. An Apparatus for the Study of In Situ Gas Evolution in Li-Ion Pouch Cells. *J Electrochem Soc* **2014**, 161 (10), A1548–A1554. <https://doi.org/10.1149/2.0151410jes>.
- (28) Zhou, F.; Zhao, X.; van Bommel, A.; Rowe, A. W.; Dahn, J. R. Coprecipitation Synthesis of $\text{Ni}_x\text{Mn}_{1-x}(\text{OH})_2$ Mixed Hydroxides. *Chemistry of Materials* **2010**, 22 (3), 1015–1021. <https://doi.org/10.1021/cm9018309>.
- (29) Wang, L.; Shi, Q.; Zhan, C.; Liu, G. One-Step Solid-State Synthesis of Ni-Rich Cathode Materials for Lithium-Ion Batteries. *Materials* **2023**, 16 (8). <https://doi.org/10.3390/ma16083079>.
- (30) Wang, L.; Huang, B.; Xiong, W.; Tong, M.; Li, H.; Xiao, S.; Chen, Q.; Li, Y.; Yang, J. Improved Solid-State Synthesis and Electrochemical Properties of $\text{LiNi}_{0.6}\text{Mn}_{0.2}\text{Co}_{0.2}\text{O}_2$ Cathode Materials for Lithium-Ion Batteries. *J Alloys Compd* **2020**, 844. <https://doi.org/10.1016/j.jallcom.2020.156034>.
- (31) Tahmasebi, M. H.; Obrovac, M. N. Quantitative Measurement of Compositional Inhomogeneity in NMC Cathodes by X-Ray Diffraction. *J Electrochem Soc* **2023**, 170 (8), 080519. <https://doi.org/10.1149/1945-7111/acefff>.